

# Modeling of diatom-diatom collisions using the Forced Harmonic Oscillator method, and high temperature kinetics applications

M. Lino da Silva, V. Guerra, J. Loureiro

Instituto de Plasmas e Fusão Nuclear, Laboratório Associado, Instituto Superior Técnico, Av. Rovisco Pais, 1049-001, Lisboa, Portugal

mลินอดาสิลวา@mail.ist.utl.pt / Fax: +351 21 841 44 55

## Abstract

This work proposes a Forced Harmonic Oscillator (FHO) based approach for the calculation of reasonably accurate vibrational transition rates in diatom-diatom collisions, for arbitrary vibrational quantum jumps over a large temperature range ( $T_{tr}=[100-100,000\text{K}]$ )

## 1 Introduction

Low-temperature ( $T_{tr} < 1000\text{K}$ ), electronically excited plasmas, have driven the research on nonequilibrium kinetic models for nearly 40 years. Comparison between numerical modeling and results obtained in this kind of plasma sources has been a driving force for progress in the determination of accurate rate databases for such applications, namely in the domain of electron-impact rates, which are capable of reproducing experimental data up to a large degree of accuracy (typically much less than one order of magnitude differences between simulation and experience). For this kind of plasmas, the effect of heavy-particles collisions has been acknowledged and modeled to a satisfactory degree, with the accounting for heavy chemical reactions and vibration-translation V-T and vibration-vibration V-V transitions, using First-Order Perturbation Theories (FOPT) such as the widespread SSH approach, coupled to a ladder-climbing assumption for heavy-impact molecular dissociation processes modeling<sup>1</sup>.

This said, the approach provided by such consolidated state-specific models has started to be challenged. New plasma sources (such as inductively coupled and microwave plasma sources) have been introduced in laboratory setups, which allow exploring higher energy domains (where gas temperatures  $T_{tr}$  in excess of 1000K are achieved). Furthermore, research on less common plasma sources (such as atmospheric entry shock-induced plasmas, or laser-induced plasmas) has matured significantly. Early attempts for simulating this new brand of plasmas, simply resorting to the simple extrapolation of the previously discussed models, showed that the obtained results became increasingly inaccurate for higher plasma energies.

### 1.1 Limits of FOPT theories for vibrational excitation and dissociation

The shortcomings of FOPT models have been discussed in other review works (see for example the Refs. [2, 3, 4]), and will only be outlined in here. FOPT models treat molecular collisions in a perturbative fashion and as such, assume that the energy defect between the two transition states is higher than the collision energy. This means that for higher collision energies, the predicted transition probability will no longer be valid, becoming increasingly higher than the “exact” transition probability, as the collision energy increases. Another consequence is that for low energy jumps (like for near-dissociative levels), the predicted transition probabilities will be overpredicted, even for temperatures as low as ambient temperature. Those lead overall to overestimated high-temperature rates. On the other side, FOPT models are not capable of calculating multiquantum transitions, which become non-negligible at higher temperatures. This in turn leads to the underprediction of the higher levels populations, and in some cases might balance the overprediction of the mono-quantum transition rates, providing a false impression of accuracy.

<sup>1</sup>See Ref. [1] for an application to the modeling of a nitrogen discharge

## 2 The FHO Method as a Bridging Approach for the Simulation of High-Temperature Vibrational Transfer and Dissociation

Present-day quantum-chemistry methods are capable of providing potential energy surfaces which accurately describe molecular interactions. The application of quasi-classical or quantum trajectory methods over such potential surfaces allows obtaining accurate state-specific datasets for any arbitrary collision energy. However, such methods remain very computationally intensive, even in the present day<sup>2</sup>. Detailed state-specific datasets are produced at a limited pace, and mostly for atom-diatom transitions [5, 6]. It is therefore useful to look into a bridging method. The Forced Harmonic Oscillator (FHO) model, being a semianalytical model that doesn't bear most of the shortcomings of FOPT models, provides such a bridging function. Table 1 shows a comparison between the three approaches.

Table 1: Comparison between FOPT, FHO, and 3D trajectories methods

	FOPT (SSH)	FHO	Classical/Quantum Trajectory Methods
Collison Trajectories	1D repulsive	1D repulsive/attractive 3D repulsive	3D
Collison Energy	perturbative (only low T)	Any	Any
energy jumps	$\Delta E_{i \rightarrow j} > \Delta E_{tr}$	Any	Any
multiquantum	No	Yes	Yes
Intermolecular Potential	Isotropic	Isotropic	Any
Transition Type	Non-reactive only	Non-reactive only	Any

c The expressions for the transition probabilities are reported in here. A more detailed description on how to deploy and apply such expressions to the calculation of complete state-specific diatom-diatom datasets is discussed in [10, 11].

– V–T transition probabilities for collinear atom-diatom non-reactive collisions are given by Kerner [7] and Treanor [8]

$$P(i \rightarrow f, \varepsilon) = i!f!\varepsilon^{i+f} \exp(-\varepsilon) \left| \sum_{r=0}^n \frac{(-1)^r}{r!(i-r)!(f-r)!\varepsilon^r} \right|^2 \quad (1)$$

with  $n = \min(i, f)$ .– V–V–T transition probabilities for collinear diatom-diatom collisions are given by Zelechow [9]

$$P(i_1, i_2 \rightarrow f_1, f_2, \varepsilon, \rho) = \left| \sum_{g=1}^n (-1)^{(i_{12}-g+1)} \times C_{g, i_2+1}^{i_{12}} C_{g, f_2+1}^{f_{12}} \varepsilon^{\frac{1}{2}(i_{12}+f_{12}-2g+2)} \exp(-\varepsilon/2) \right. \\ \left. \times \sqrt{(i_{12}-g+1)!(f_{12}-g+1)!} \exp[-i(f_{12}-g+1)\rho] \times \sum_{l=0}^{n-g} \frac{(-1)^l}{(i_{12}-g+1-l)!(f_{12}-g+1-l)!l!\varepsilon^l} \right|^2 \quad (2)$$

with  $i_{12} = i_1 + i_2$ ,  $f_{12} = f_1 + f_2$ ,  
and  $n = \min(i_1 + i_2 + 1, f_1 + f_2 + 1)$ .

<sup>2</sup>particularly for diatom-diatom transitions

In these equations  $\varepsilon$  and  $\rho$  are related to the two-state FOPT transition probabilities, with  $\varepsilon = P_{\text{FOPT}}(1 \rightarrow 0)$  and  $\rho = [4 \cdot P_{\text{FOPT}}(1, 0 \rightarrow 0, 1)]^{1/2}$ . Finally,  $C_{ij}^k$  is a transformation matrix calculated according to the expression

$$C_{ij}^k = 2^{-n/2} \binom{k}{i-1}^{-1/2} \binom{k}{j-1}^{1/2} \times \sum_{v=0}^{j-1} (-1)^v \binom{k-i+1}{j-v-1} \binom{i-1}{v}. \quad (3)$$

## 2.1 Validation of the FHO method and comparison with the FOPT method

Some sample results for  $\text{N}_2\text{-N}_2$  collisions, outlining the reliability of the FHO model, are shortly summarized here. Fig. 1 shows a comparison between results obtained with three different approaches (FOPT, FHO, and Quantum-Classical). We see that the FHO theory reproduces well the more detailed Quantum-Classical results, with a correct behavior in the high-temperature limit. This is no longer the case of the FOPT results, that quickly diverge starting at 2,000K, until they become superior to the gas kinetic rate around 10,000K. Few experimental validations exist yet for diatom-diatom vibrational transitions, but one may verify that the calculated FHO dissociation rates have a good behavior in the Boltzmann equilibrium limit.

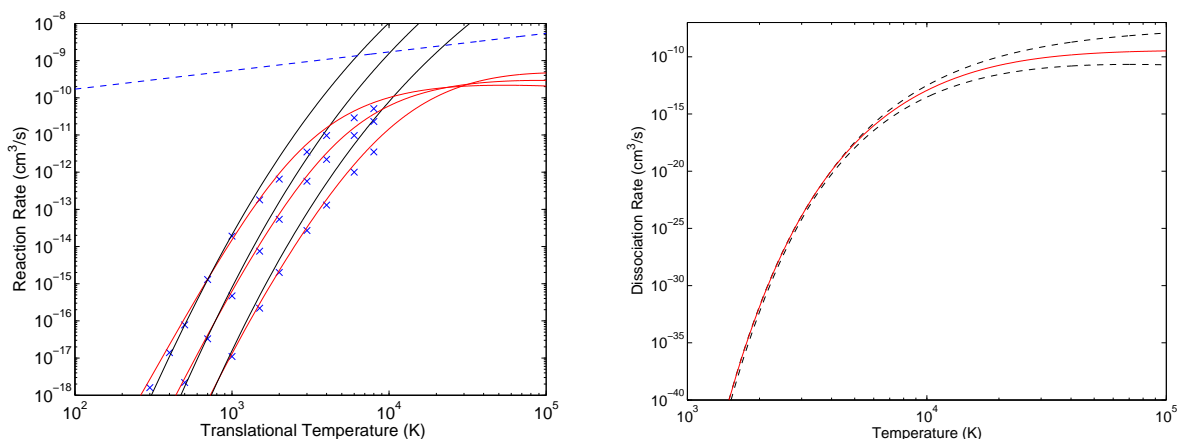


Figure 1: **Left:** Single-quantum V–T rates for  $\text{N}_2\text{-N}_2$ : —, FHO model; —, FOPT model;  $\times$ , calculations of Ref. [12]. V–T transitions  $1 \rightarrow 0$  and  $20 \rightarrow 19$  displayed from bottom to up. —, gas-kinetic collision rate. **Right:** Comparison of the reduced thermal dissociation rate of the FHO dataset for  $\text{N}_2\text{-N}_2$  collisions and the upper/lower bounds of experimental rates.

## 3 A Detailed Multiquantum Vibrationally-Specific Model for Air

A detailed state-specific multiquantum model has been produced for the simulation of heavy-impact processes for any arbitrary translational temperature. Every-time more detailed results from full 3D trajectory models are available, these are used in our model. Then the remaining transitions are produced using the state-to-state model. We therefore consider non-reactive and reactive atom-diatom V–T and V–D rates from the Bari team [5, 6], both for nitrogen and oxygen-containing mixtures. Then we complete these datasets with our own datasets for nonreactive diatom-diatom V–T and V–D transitions for these same mixtures. For Zeldovich transitions involving NO, we consider the dataset of reactive atom-diatom rates from Bose and Candler [14, 15], which we complete by a non-reactive atom-diatom and diatom-diatom dataset for collisions with NO, obtained using the FHO model. The required isotropic potential energy surface parameters are estimated from more detailed PES published in the literature [16, 17].

Table 2 outlines this detailed multiquantum dataset, listing the different 22 transitions, and the method that has been utilized for determining the corresponding rates, as well as the corresponding FHO potential parameters, when applicable.

Table 2: T–V–E dataset reactions, models, and parameters

No.	Reaction	Model	$\alpha^{-1}$ (Å)	E (K)	Ref.
1	$\text{N}_2(\text{X},v_i) + \text{N}_2 \rightleftharpoons \text{N}_2(\text{X},v_f) + \text{N}_2$	FHO	4	200	[10]
2	$\text{N}_2(\text{X},v_i) + \text{N}_2 \rightleftharpoons \text{N} + \text{N} + \text{N}_2$	FHO	4	200	[10]
3	$\text{N}_2(\text{X},v_i) + \text{O}_2 \rightleftharpoons \text{N}_2(\text{X},v_f) + \text{O}_2$	FHO	4	200	[10]
4	$\text{N}_2(\text{X},v_i) + \text{O}_2 \rightleftharpoons \text{N} + \text{N} + \text{O}_2$	FHO	4	200	[10]
5	$\text{O}_2(\text{X},v_i) + \text{N}_2 \rightleftharpoons \text{O}_2(\text{X},v_f) + \text{N}_2$	FHO	4	200	[10]
6	$\text{O}_2(\text{X},v_i) + \text{N}_2 \rightleftharpoons \text{O} + \text{O} + \text{N}_2$	FHO	4	200	[10]
7	$\text{O}_2(\text{X},v_i) + \text{O}_2 \rightleftharpoons \text{O}_2(\text{X},v_f) + \text{O}_2$	FHO	4	380	[13]
8	$\text{O}_2(\text{X},v_i) + \text{O}_2 \rightleftharpoons \text{O} + \text{O} + \text{O}_2$	FHO	4	380	[13]
9	$\text{N}_2(\text{X},v_i) + \text{N} \rightleftharpoons \text{N}_2(\text{X},v_f) + \text{N}$	QCT	–	–	[5]
10	$\text{N}_2(\text{X},v_i) + \text{N} \rightleftharpoons \text{N} + \text{N} + \text{N}$	QCT	–	–	[5]
11	$\text{O}_2(\text{X},v_i) + \text{O} \rightleftharpoons \text{O}_2(\text{X},v_f) + \text{O}$	QCT	–	–	[6]
12	$\text{O}_2(\text{X},v_i) + \text{O} \rightleftharpoons \text{O} + \text{O} + \text{O}$	QCT	–	–	[6]
13	$\text{N}_2(\text{X},v_i) + \text{O} \rightleftharpoons \text{N}_2(\text{X},v_f) + \text{O}$	FHO*	–	–	[14]
14	$\text{N}_2(\text{X},v_i) + \text{O} \rightleftharpoons \text{N} + \text{N} + \text{O}$	FHO*	–	–	[14]
15	$\text{O}_2(\text{X},v_i) + \text{N} \rightleftharpoons \text{O}_2(\text{X},v_f) + \text{N}$	FHO*	–	–	[15]
16	$\text{O}_2(\text{X},v_i) + \text{N} \rightleftharpoons \text{O} + \text{O} + \text{N}$	FHO*	–	–	[15]
17	$\text{N}_2(\text{X},v_i) + \text{O} \rightleftharpoons \text{NO}(\text{X},v_f) + \text{N}$	QCT	–	–	[14]
18	$\text{O}_2(\text{X},v_i) + \text{N} \rightleftharpoons \text{NO}(\text{X},v_f) + \text{O}$	QCT	–	–	[15]
19	$\text{NO}(\text{X},v_i) + \text{N}_2 \rightleftharpoons \text{NO}(\text{X},v_f) + \text{N}_2$	FHO	4	200	[16]
20	$\text{NO}(\text{X},v_i) + \text{N}_2 \rightleftharpoons \text{N} + \text{O} + \text{N}_2$	FHO	4	200	[16]
21	$\text{NO}(\text{X},v_i) + \text{O}_2 \rightleftharpoons \text{NO}(\text{X},v_f) + \text{O}_2$	FHO	4	380	[17]
22	$\text{NO}(\text{X},v_i) + \text{O}_2 \rightleftharpoons \text{N} + \text{O} + \text{O}_2$	FHO	4	380	[17]

## References

- [1] Guerra, V., Sá, P. A., and Loureiro, J. 2004 *Eur. Phys. J. Appl. Phys.* 28 125.
- [2] Capitelli, M., Armenise, I., Bruno D., Cacciatore, M., Celiberto, R., Colonna, G., De Pascale, O., Diomede, P., Esposito, F, Gorse, C., Hassouni, K., Laricchiuta, A., Longo, S., Pagano, D., Pietanza, D., Rutigliano, M. 2007 *Plasma Sources Sci. Technol.* 16 S30.
- [3] Capitelli, M., Celiberto, R., Esposito, F. and Laricchiuta, A. 2009 *Plasma Processes Polym.* 6 279–294.
- [4] Lino da Silva M. Guerra V. and Loureiro J. 2009 *Plasma Sources Sci. Technol.* 18 034023.
- [5] Esposito, F., Armenise, I., and Capitelli, M. 2006 *Chem. Phys.* 331 1.
- [6] Esposito, F., Armenise, I., Capitta, G.. and Capitelli, M. 2008 *Chem. Phys.* 351 91.
- [7] Kerner, E. H. 1958 *Can. J. Phys.* 36(3) 371.
- [8] Treanor, C. E. 1965 *J. Chem. Phys.* 43(2) 532.
- [9] Zelechow, A., Rapp, D., and Sharp, T. E. 1968 *J. Chem. Phys.* 49(1) 286.
- [10] Adamovich, I. V., Macheret, S. O., Rich, J. W., and Treanor, C. E. 1998 *J. Thermophys. Heat Transfer* 12 57.
- [11] Lino da Silva M. Guerra V. and Loureiro J. 2007 *J. Thermophys. Heat Transfer* 21(1) 40.
- [12] Billing, G. D., Fisher, E. R. 1979 *Chem. Phys.* 43(3) 395.
- [13] Lino da Silva, M., Guerra, V., and Loureiro, J. 2012 *Chem. Phys. Lett.* 531, 28–3.
- [14] Bose, D., and Candler, G. V. 1996 *J. Chem. Phys.* 104(8) 1996 2825.
- [15] Bose, D., and Candler, G. V. 1996 *J. Chem. Phys.* 107(8) 1996 6136.
- [16] Bartolomei, M., Cappelletti, D., de Petris, G., Teixidor, M. M., Pirani, F., Rosi, M., and Vecchiocattivi, F. 2008 *Phys. Chem. Chem. Phys.* 10(39) 5993.
- [17] Bacon, J. A., Giese, C. F., and Gentry, W. R., 1998 *J. Chem. Phys.* 108(8) 3127.